International Journal of Numerical Methods for Heat & Fluid Flow

Impact of partial slip on mixed convective flow towards a Riga plate comprising micropolar TiO_2-kerosene/water nanoparticles

Aurang Zaib, Rizwan Ul Haq, Ali J. Chamkha, Mohammad Mehdi Rashidi,

Impact of partial slip on mixed convective flow towards a Riga plate comprising micropolar TiO_2-kerosene/water nanoparticles

Received 1 June 2018
Revised 6 August 2018
Accepted 23 August 2018

Aurang Zaib
Department of Mathematical Sciences, Federal Urdu University of Arts, Science and Technology Karachi, Karachi, Pakistan

Rizwan Ul Haq
Department of Electrical Engineering, Bahria University Islamabad, Islamabad, Pakistan

Ali J. Chamkha
Department of Mechanical Engineering, Prince Mohammad Bin Fahd University, Al-Khobar, Saudi Arabia and RAK Research and Innovation Center, American University of Ras Al Khaimah, Ras Al Khaimah, United Arab Emirates, and

Mohammad Mehdi Rashidi
Department of Civil Engineering, University of Birmingham, Birmingham, UK

Abstract

Purpose – The purpose of this paper is to present an inclusive study of the mixed convective flow involving micropolar fluid holding kerosene/water-based TiO_2 nanoparticle towards a vertical Riga surface with partial slip. The outcomes are confined for opposing and assisting flows.

Design/methodology/approach – Similarity equations are acquired and then worked out numerically by the Keller box technique.

Findings – Impacts of significant parameters on microrotation velocity, temperature distribution, velocity profile together with the Nusselt number and the skin friction are argued with the help of graphs. Two solutions are achieved in opposing flow, while the solution is unique in assisting flow. It is also monitored that the separation of boundary layer delays because of micropolar parameter and accelerates because of volume fraction.

Originality/value – The authors trust that all these results are new and significant for researchers.

Keywords Micropolar fluid, mix convection, partial slip, TiO_2 nanoparticle.

Paper type Research paper

Nomenclature

b, c = positive constants;
C_{fx} = skin friction coefficient;
C_p = specific heat of fluid;
d = electrodes and magnets width;
g = acceleration caused by gravity;

International Journal of Numerical Methods for Heat & Fluid Flow
© Emerald Publishing Limited
0961-5539
DOI 10.1108/HFF-06-2018-0258

Gr_x = Grash of number;
J_O = applied current density in the electrodes;
j = micro inertia density;
K = micropolar parameter;
$\breve{\kappa}$ = vortex viscosity;
$\breve{k}_f$ = thermal conductivity of regular liquid;
$\breve{k}_s$ = thermal conductivity of nanoliquid;
$\breve{M}_0$ = magnetization of the permanents magnets;
$\breve{N}$ = micro rotation vector;
$\breve{n}$ = micro gyration parameter;
Nu_x = Nusselt number;
Pr = Prandtl number;
Re_x = local Reynolds number;
$\breve{T}$ = temperature;
$\breve{T}_\infty$ = free stream temperature;
$\breve{T}_w$ = fluid temperature at wall;
$\breve{u}_\infty$ = free stream velocity;
$\breve{u}, \breve{v}$ = velocity components; and
$\breve{x}, \breve{y}$ = Cartesian coordinates.

Greek symbols
α = modified Hartmann number;
$\breve{\alpha}_{nf}$ = thermal diffusivity;
β_{nf} = nanofluid thermal expansion;
ε = slip length;
γ = slip parameter;
$\breve{\gamma}_{nf}$ = spin-gradient viscosity;
$\breve{\kappa}$ = vortex viscosity;
λ = mixed convective parameter;
$\breve{\mu}_{nf}$ = nanofluid dynamic viscosity;
ϕ = volume fraction of nanoliquid;
θ = dimensionless temperature;
v_f = kinematic viscosity;
$\breve{\rho}_{nf}$ = density;
$\breve{\rho}_s$ = density of nanoliquid;
$\breve{\rho}_f$ = density of base fluid;
ψ = stream function;
Λ = dimensionless parameter; and
η = similarity variable.

Subscripts
w = condition at wall; and
∞ = condition at free stream.

Superscripts
$'$ = derivative w.r.t. η.

Introduction

In modern time, to enhance the capabilities of heat transfer of regular fluids such as engine oil, water and glycerin because of the weaknesses of the thermal properties, nanofluid is the excellent gift to improve the thermal conductivity. Nanofluid is a fluid which is constructed by dispersion of nano-meter-sized solid particles and/or fibers having diameter below 100 nm. To fulfill the lofty demands of industrial fields, nanofluids are used in many processes such as targeted drug delivery, extraction of geothermal forces, propellant combustion, cooling of automotive engine, heat exchanger, etc. Choi (1995) was first who used the concept of nanofluid. He showed experimentally that the properties of thermal characteristics can be increased by dispersing the nanoparticle into the regular liquids. Pak and Cho (1998) discussed experimentally the turbulent flow of two kinds of nanoparticles, namely, titanium dioxide and γ-alumina. They clarified that the coefficients of convective heat transfer of water improved via dispersing nanoparticles. Eastman *et al.* (1999) explored an experiment on water-based copper nanoparticle and found that the coefficient of heat transfer was higher than pure water. Gorla *et al.* (2011) scrutinized the boundary layer flow with heat transfer comprising nanofluid over a stretched circular cylinder. Makinde and Aziz (2011) obtained the numerical result of flow containing nanoparticle over a stretched sheet with thermal convective condition. Nohgrehabadi *et al.* (2012a) explored the influence of slip effect on flow comprising nanoliquid past a stretched surface. The impact of free convective flow containing microorganisms and nanopaticle towards a horizontal surface immersed in a porous medium was scrutinized by Aziz *et al.* (2012). Motsumi and Makinde (2012) discussed the impact of thermal radiation on fluid flow holding nanofluid from a moving porous plate with viscous dissipation. Nohgrehabadi *et al.* (2012b) explored the impact of MHD on viscous flow containing nanomaterial past an isothermal stretched surface. The stagnation-point flow past a permeable stretched sheet comprising nanofluid was investigated by Alsaedi *et al.* (2012). Rashad *et al.* (2013) discussed the impact of mixed convective flow involving non-Newtonian nanoliquid through a vertical sheet embedded in porous medium. Free convective flow containing nanomaterial through vertical cone in non-Darcy porous medium was investigated by Nohgrehabadi *et al.* (2013a). Nohgrehabadi *et al.* (2013b) scrutinized the slip flow with heat transfer comprising nanoliquid towards a stretched surface with convective boundary condition. The influence of entropy analysis on flow of nanoliquid from a stretched surface with slip effect and heat generation/absorption was discussed by Nohgrehabadi *et al.* (2013c). Nadeem *et al.* (2014) explored the influences of elasticity and MHD on two-dimensional flow of Maxwell liquid comprising nanofluid from a stretched sheet. Chamkha and Rashad (2014) explored the influence of MHD on forced convective flow comprising nanoparticle from a non-isothermal wedge. Natural convective flow over a vertical plate containing nanofluid in porous medium with convective boundary condition was investigated by Ghalambaz *et al.* (2014). El-Kabeir *et al.* (2015) analyzed the influence of partial slip on unsteady flow holding nanofluid through a contracting cylinder in the presence of Newtonian heating. Impacts of Dufour and Soret effects on mixed convective flow containing nanoliquid past a nonlinear stretched surface with radiation effect were scrutinized by Pal *et al.* (2016). Ahmed and Rashad (2016) considered the natural convective flow involving micropolar fluid holding nanoparticle in a rectangular enclosure embedded in anisotropic porous medium and obtain the numerical solution via finite volume method. Ghalambaz *et al.* (2016) considered the combined effects of radiation and viscous dissipation on free convective flow holding nanoliquid from a square cavity in porous medium. Influence of partial slip on MHD mixed convective flow comprising water-based copper nanoparticle from two sided lid driven porous cavity was scrutinized by Sivasankaran *et al.* (2016). Rashad (2017b) scrutinized the unsteady slip flow holding nanofluid from an inclined convectively-heated stretched sheet. In other paper, Rashad (2017a) discussed the combined effects of partial slip and thermal radiation on mixed convective flow containing cobalt-kerosene ferroliquid from a non-isothermal wedge. Zargartalebi *et al.* (2017) studied the unsteady natural convective flow through porous cavity via finite conducting walls by taking thermal non-equilibrium and time periodic conditions. Mustafa *et al.* (2017) analyzed the influence of chemical reaction on mixed convective flow holding nanofluid from stretched sheet with activation energy and magnetic field. Recently, Tahmasebi *et al.* (2018) modeled the free convective flow filled with porous cavity involving nanomaterial with three types of layers.

Because of practical significance, the influences of non-Newtonian liquids are the leading interest of researchers in the arena of science and technology. Such liquids generally arise in several processes for instance printing of ink jet coating, products of food and cosmetic, volcanic lava, process of polymer, fluid crystals, geological flows, suspensions of colloidal flows and numerous other processes. There are numerous mathematical models exist in the literature with several constitutive equations containing many empirical parameters. Micropolar liquid holds the suspensions of dilute of macro-molecules rigid with motions of individual to sustain body moments and stress which are concerned through spin inertia. Eringen (1966) developed this theory that compact fluids class which show certain character of micro-scope occurring from fluid elements local structure and the micro-rotation. Since then, amount of significant research on micropolar fluid (Kelson and Farrell, 2001; El-Arabawy, 2003; Abo-Eldahab and El-Aziz, 2005; Hayat *et al.*, 2009; Ashraf and Bashir, 2012; Das, 2012a; Zaib *et al.*, 2016; Waqas *et al.*, 2016) under several conditions with different physical aspects has been reported. There are number of situations where it is necessary to change the no-slip condition with slip condition because when liquid moves in MEMS (micro-electro mechanical) system, the no slip condition is no longer exist at the solid-liquid interface. The area of non-equilibrium is more precisely portrayed through the model of slip flow near an interface. Wang (2009) obtained the solution in closed form of viscous flow from a permeable stretched sheet with partial slip. The impact of partial slip on flow from a shrinking porous surface was explored by Aman and Ishak (2010). Das (2012b) scrutinized the influence of partial slip on mixed convective flow involving micropolar fluid from a shrinking surface with magnetic field. The electrically conducting flow on heat transfer of second grade liquid through channel with partial slip was investigated by Ellahi and Hameed (2012). Zaib and Shafie (2015) discussed the unsteady flow towards a stagnation-point containing micropolar fluid from a shrinking sheet with thermophoresis. Recently, Shah *et al.* (2017) explored the impact of magnetic field on heat transfer of Carreau fluid from a stretched sheet with radiation, erratic thermal conductivity and dissipation in porous medium.

Impacts of Electro–magneto–hydrodynamic (EMHD) through fluid flows play an elementary role in performance of momentum and the significance observed in thermal reactor, micro-coolers, controlling the flow in network of fluidic and chromatography of liquid. Initial studies showed that Gailitis and Lielausis (1961) introduced the device to control the flow known as Riga plate. This device is an actuator of electro-magnetic and it holds magnets permanently; it is useful to decline the drag of pressure a continuous boundary layer separation. Pantokratoras and Magyari (2009) scrutinized the impact of EMHD on natural convective flow through a Riga plate. The classical Sakiadis and Blasius problems were discussed via Riga plate by Pantokratoras (2011) and acquired the numerical solution by finite difference technique. Ahmad *et al.* (2016) discussed the mixed convective flow containing nanofluid from a Riga plate and achieved the analytic solution via perturbation technique. Iqbal *et al.* (2017) scrutinized the influence of melting heat transfer towards a stagnation-point comprising nanoliquid from a Riga plate with irregular thickness and thermal radiation.

Recently, Iqbal *et al.* (2018) inspected the combined effects of viscous dissipation and thermal radiation on flow of Casson fluid from a stretched Riga plate with heat generation.

The current investigation adds a novel era for researchers to discover the characteristics of non-Newtonian nanofluid. Therefore, we investigate the mixed convective flow containing micropolar TiO_2-kerosene/water nanoparticles past a Riga plate with partial slip. Similarity equations are developed and obtained dual numerical solutions via the Keller box technique. The impacts of the important parameters are argued in detail by tables and graphs.

Problem formulation

We consider a steady mixed convective flow of micropolar liquid holding TiO_2-kerosene/water nanoparticle near a stagnation-point from a Riga plate with partial slip. We presume that the free stream velocity is $\breve{u}_\infty(\breve{x}) = c\breve{x}$ and wall temperature $\breve{T}_w(\breve{x}) = \breve{T}_\infty + b\breve{x}$ vary linearly, where c and b are positive constants and $\breve{T}_\infty$ is ambient temperature. Further, Riga plate contains the permanent magnets and an irregular array of electrodes accumulated on the surface of plate (Figure 1). The governing equations in such assumptions through the usual boundary layer and the Boussinesq approximation are written as:

$$\frac{\partial \breve{u}}{\partial \breve{x}} + \frac{\partial \breve{v}}{\partial \breve{y}} = 0 \tag{1}$$

$$\breve{u}\frac{\partial \breve{u}}{\partial \breve{x}} + \breve{v}\frac{\partial \breve{u}}{\partial \breve{y}} - \breve{u}_\infty\frac{d\breve{u}_\infty}{d\breve{x}} = \frac{1}{\breve{\rho}_{nf}}\left(\breve{\mu}_{nf} + \breve{\kappa}\right)\frac{\partial^2 \breve{u}}{\partial \breve{y}^2} + \frac{\breve{\kappa}}{\breve{\rho}_{nf}}\frac{\partial \breve{N}}{\partial \breve{y}} + \frac{\pi \breve{J}_0 \breve{M}_0}{8\breve{\rho}_{nf}}e^{-\frac{\pi}{d}\breve{y}} + \frac{g(\rho\beta)_{nf}}{\breve{\rho}_{nf}}\left(\breve{T} - \breve{T}_\infty\right) \tag{2}$$

$$\breve{u}\frac{\partial \breve{N}}{\partial \breve{x}} + \breve{v}\frac{\partial \breve{N}}{\partial \breve{y}} = \frac{\breve{\gamma}_{nf}}{\breve{\rho}_{nf}j}\frac{\partial^2 \breve{N}}{\partial \breve{y}^2} - \frac{\breve{\kappa}}{\breve{\rho}_{nf}j}\left(2\breve{N} + \frac{\partial \breve{u}}{\partial \breve{y}}\right), \tag{3}$$

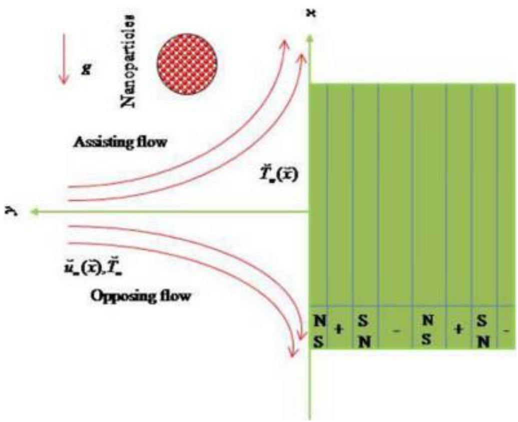

Figure 1. Physical diagram of the problem

$$\breve{u}\frac{\partial \breve{T}}{\partial \breve{x}} + \breve{v}\frac{\partial \breve{T}}{\partial \breve{y}} = \breve{\alpha}_{nf}\frac{\partial^2 \breve{T}}{\partial \breve{y}^2}, \tag{4}$$

The physical boundary conditions are:

$$\begin{gathered}\breve{u} = \varepsilon\breve{\mu}_{nf}\frac{\partial \breve{u}}{\partial \breve{y}},\ \breve{N} = -\breve{n}\frac{\partial \breve{u}}{\partial \breve{y}},\ \breve{v} = 0,\ \breve{T} = \breve{T}_w(\breve{x}) \text{ at } \breve{y} = 0,\\ \breve{u} \to \breve{u}_\infty(\breve{x}),\ \breve{T} \to \breve{T}_\infty,\ \breve{N} \to 0 \text{ as } \breve{y} \to \infty.\end{gathered} \tag{5}$$

where $\breve{v}, \breve{u}$ are the components of velocity in $\breve{y}-$ and $\breve{x}-$directions, respectively, $\breve{\rho}_{nf}$, $\breve{\mu}_{nf}$, $\breve{\kappa}$, $\breve{M}_0$, d, J_0, g, β_{nf} are the nanofluid density, nanofluid dynamic viscosity, vortex viscosity, magnetization of the permanents magnets, electrodes and magnets width, the applied current density in the electrodes, acceleration caused by gravity and nanofluid thermal expansion, respectively; ε, $\breve{N}$, $\breve{T}$, $\breve{\gamma}_{nf}$, $\breve{\alpha}_{nf}$, j, $\breve{n}$ are slip length, micro rotation vector, temperature, thermal diffusivity, spin gradient viscosity, micro inertia density and micro gyration parameter, respectively. It is well-known that the micro gyration parameter varies as $0 \le \breve{n} \le 1$, where $\breve{n} = 0$ represents strong concentration; for $\breve{n} = 0.5$ signifies as weak concentration and $\breve{n} = 1$ indicates turbulent flow.

The values of $\breve{\rho}_{nf}$, $\breve{\alpha}_{nf}$, $(\rho c_p)_{nf}$, $\breve{\mu}_{nf}$, k_{nf}/k_f, $\breve{\gamma}_{nf}$, $(\breve{\rho}\ \breve{\beta})_{nf}$ are classified as (Rashid *et al.*, 2017; Hussanan *et al.*, 2018):

$$\breve{\rho}_{nf} = (1-\phi)\breve{\rho}_f + \phi\breve{\rho}_s,\ \breve{\alpha}_{nf} = \breve{k}_{nf}/(\breve{\rho}\ \breve{c}_p)_{nf},$$

$$(\breve{\rho}\ \breve{c}_p)_{nf} = (1-\phi)(\breve{\rho}\ \breve{c}_p)_f + \phi(\breve{\rho}\ \breve{c}_p)_s,$$

$$\breve{\mu}_{nf} = \frac{\breve{\mu}_f}{(1-\phi)^{2.5}},\ \frac{\breve{k}_{nf}}{\breve{k}_f} = \frac{(\breve{k}_s + 2\breve{k}_f) - 2\phi(\breve{k}_f - \breve{k}_s)}{(\breve{k}_s + 2\breve{k}_f) + \phi(\breve{k}_f - \breve{k}_s)},$$

$$\breve{\gamma}_{nf} = (\breve{\mu}_{nf} + \breve{\kappa}/2), \qquad (\breve{\rho}\ \breve{\beta})_{nf} = (1-\phi)(\breve{\rho}\ \breve{\beta})_f + \phi(\breve{\rho}\ \breve{\beta})_s. \tag{6}$$

where ϕ, $\breve{k}_f$, $\breve{k}_s$, $\breve{\rho}_s$, $\breve{\rho}_f$, $(\breve{\rho}\ \breve{\beta})_s$ and $(\breve{\rho}\ \breve{\beta})_f$ are the volume fraction of nanoliquid, the thermal conductivity of regular liquid, thermal conductivity of nanoliquid, density of nanoliquid, density of base fluid, coefficients of thermal expansion of nanoliquid and base fluid, respectively.

We use the similarity transformation:

$$\begin{gathered}u = c\breve{x}F'(\eta),\ \eta = y\sqrt{\frac{c}{\nu_f}},\ v = -\sqrt{c\nu_f}F(\eta),\\ \breve{N}(\eta) = c\breve{x}\sqrt{\frac{c}{\nu_f}}\breve{G},\ \theta(\eta) = \frac{\breve{T} - \breve{T}_\infty}{\breve{T}_w - \breve{T}_\infty}.\end{gathered} \tag{7}$$

In view of Equation (7), Equations (2)-(5) using Equation (6) are transmuted to:

$$\left(\frac{1+(1-\phi)^{2.5}K}{(1-\phi)^{2.5}}\right)F''' + \left[(1-\phi)+\phi\frac{\breve{\rho}_s}{\breve{\rho}_f}\right](FF''-F'^2+1)+KG' + \alpha e^{-\Lambda\eta} + \lambda\left[(1-\phi)+\phi\frac{(\breve{\rho}\breve{\beta})_s}{(\breve{\rho}\breve{\beta})_f}\right]\theta = 0 , \quad (8)$$

$$\left(\frac{2+(1-\phi)^{2.5}K}{2(1-\phi)^{2.5}}\right)G'' + \left[(1-\phi)+\phi\frac{\breve{\rho}_s}{\breve{\rho}_f}\right](fG'-f'G)-K(2G+F'')=0, \quad (9)$$

$$\frac{(\breve{k}_s+2\breve{k}_f)-2\phi(\breve{k}_f-\breve{k}_s)}{(\breve{k}_s+2\breve{k}_f)+\phi\left(\breve{k}_f-\breve{k}_s\right)}\theta'' + \Pr\left[(1-\phi)+\phi\frac{(\breve{\rho}\,\breve{c}_p)_s}{(\breve{\rho}\,\breve{c}_p)_f}\right](F\theta'-F'\theta)=0, \quad (10)$$

With the converted boundary conditions:

$$F(0)=0,\ G(0)=-\breve{n}\,F''(0),\ F'(0)=\frac{\gamma}{(1-\phi)^{2.5}}F''(0),\ \theta(0)=1 \text{ at } \eta=0,$$

$$F'(\infty)\to 1,\ \theta(\infty)\to 0,\ G(\infty)\to 0 \text{ as } \eta\to\infty. \quad (11)$$

In above equations, the dimensions less constants are micropolar parameter K, mixed convective parameter λ, Re_x Reynolds number, γ slip parameter, α modified Hartmann number, Λ dimensionless parameter and Pr Prandtl number are described as:

$$K=\breve{\kappa}/\breve{\mu}_f,\quad \lambda=\breve{\beta}_f gb/c^2 = Gr_x/\mathrm{Re}_x^2,\quad Gr_x = g\breve{\beta}_f(T_w-T_\infty)\breve{x}^3/\nu_f^2,\quad \mathrm{Re}_x=\breve{x}\,\breve{u}_e(\breve{x})/\nu_f,$$

$$\gamma=\varepsilon\breve{\mu}_f\sqrt{c/v_f},\ \alpha=\pi J_0M_0/8c^{3/2}\,\mathrm{Re}_x^{1/2}\breve{\rho}_f\sqrt{v_f},\ \Lambda=\pi\sqrt{v_f}/d\sqrt{c},\ \Pr=\nu_f\left(\breve{\rho}\,c_p\right)_f/\breve{k}_f,$$

$$j=\nu_f/c.$$

The coefficient of skin friction and the Nusselt number are:

$$C_{fx}=\frac{1}{\breve{\rho}_{nf}\breve{u}_\infty^2}\left[(\breve{\mu}_{nf}+\breve{\kappa})\frac{\partial\breve{u}}{\partial\breve{y}}+\breve{\kappa}\,\breve{N}\right]_{\breve{y}=0},\ Nu_x=-\frac{\breve{x}\,\breve{k}_{nf}}{\breve{k}_f(\breve{T}_w-\breve{T}_\infty)}\frac{\partial\breve{T}}{\partial\breve{y}}\bigg|_{\breve{y}=0} \quad (12)$$

Using Equations (6) and (7), we obtain:

$$C_{fx}\,\mathrm{Re}_x^{1/2} = \frac{1}{\left[(1-\phi)+\phi\frac{\breve{\rho}_s}{\breve{\rho}_f}\right]}\left(\frac{1+(1-\phi)^{2.5}(1-\breve{n})K}{(1-\phi)^{2.5}}\right)F''(0),\; Nu_x\,\mathrm{Re}_x^{-1/2} = -\frac{k_{nf}}{k_f}\theta'(0) \tag{13}$$

Results and discussions

Equations (8)-(10) through boundary condition in Equation (11) are computed numerically via the Keller-box technique. This following argument is based on the watchful investigation of Figures expressing the influence of TiO_2 nanoparticle existence in the regular fluids (kerosene/water) for different values of the dimensionless parameters. Here, we considered the micro gyration parameter $n = 0.5$. It is worth mentioning that the dual solutions are obtained by setting different values of boundary layer thicknesses η_∞. For the first solution $\eta_\infty \approx 5$, however in case of second solution, the boundary layer thickness enhances, that is, $\eta_\infty \approx 8$. The properties of thermo-physical for regular liquids and particle are illustrated in Table I. In Tables II and III, we judged our results of $F''(0)$ and $-\theta'(0)$ with available outcomes and found to be in tremendous agreement.

Figures 2(a)-(c) show the impact of nanoparticle volume fraction on the velocity, micro rotation profiles and temperature distribution for water-based nanofluid. It is scrutinized from Figure 2(a) that the velocity of fluid shrinks when ϕ climbs in first solution while the profile increases in second solution. Because of nanoparticle volume fraction, the thermal

Table I.
Thermo physical properties of base fluids and TiO_2

	Base fluids		
Material	Water	Kerosene	TiO_2
$C_p(J/kgK)$	4179	2090	686.2
$\rho(kg/m^3)$	997.1	783	4250
$k(W/mK)$	0.613	0.145	8.9538
$\beta \times 10^{-5}(1/K)$	21	99	0.9
Pr	6.2	21	–

Table II.
Comparison of $f''(0)$ when $\lambda = 1$, $\phi = 0$; $K = 0$

Pr	Lok *et al.* (2006)	Aman *et al.* (2011)	Present
0.7	1.7064	1.7063	1.7063
1	–	1.6754	1.6754
7	1.5180	1.5179	1.5179
10	–	1.4928	1.4928
20	1.4486	1.4485	1.4485
40	1.4102	1.4101	1.4101
50	–	1.3989	1.3989
60	1.3903	1.3903	1.3903
80	1.3773	1.3773	1.3776
100	1.3677	1.3680	1.3683

conductivity raises which in turns thinning the velocity boundary layer. In contrast, the profile of micro rotation shows a rising behavior in both solutions as depicted in Figure 2(b). In contrast, the temperature distribution [Figure 2(c)] lifts with ϕ for first solution and drops in second solution. Physically as nanoparticle volume fraction of TiO_2 develops the thermal conductivity which consequently boosts the thickness of thermal boundary layer in first solution. Alterations in the shape, size, material and nanoparticle volume fraction permits for modification to maximize absorption of energy via the volume of fluid, as the nanoparticle volume fraction depends on the size of the particle. Enhancing of volume fraction nanoparticle, results in climbing of coefficient of heat transfer.

The influence of slip parameter γ on velocity, micro rotation profiles and temperature distribution are portrayed in Figures 3(a)-(c) for water-based nanofluid. Figure 3(a) suggests that the velocity profile grows with larger values of γ in first solution and consequently

Pr	Lok et al. (2006)	Aman et al. (2011)	Present
0.7	0.7641	0.7641	0.7641
1	–	0.8708	0.8708
7	1.7226	1.7224	1.7224
10	–	1.9446	1.9446
20	2.4577	2.4476	2.4576
40	3.1023	3.1011	3.1011
50	–	3.3415	3.3415
60	3.5560	3.5514	3.5515
80	3.9195	3.9095	3.9097
100	4.2289	4.2116	4.2120

Table III. Comparison of $-\theta'(0)$ when $\lambda = 1, \phi = 0, K = 0$

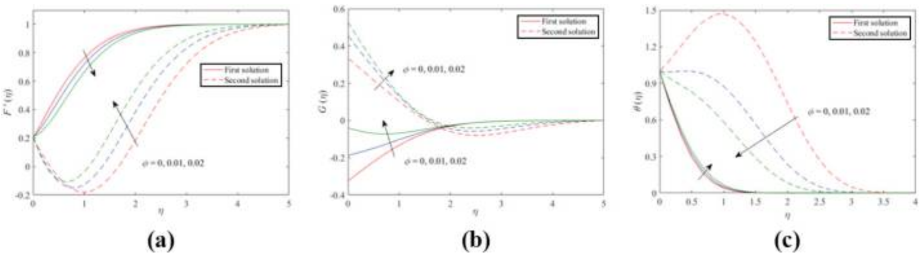

Figure 2. Impact of ϕ on (a) $F'(\eta)$ (b) $G(\eta)$ and (c) $\theta(\eta)$ when $K = 0.5$, $\gamma = 0.2$, $\lambda = -1.5$, $\alpha = 0.1$, $\Lambda = 1$

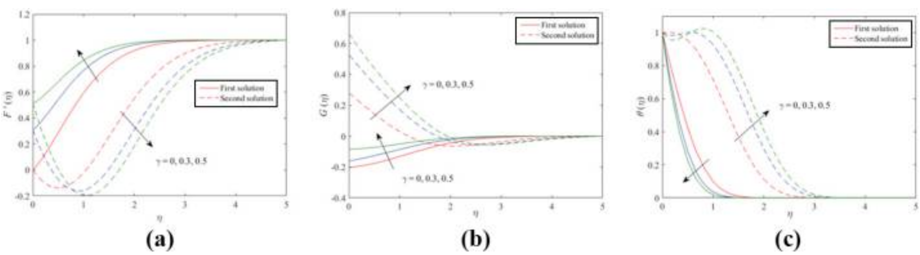

Figure 3. Impact of γ on (a) $F'(\eta)$ (b) $G(\eta)$ and (c) $\theta(\eta)$ when $\phi = 0.01$, $K = 0.5$, $\lambda = -1.5$, $\alpha = 0.1$, $\Lambda = 1$

shrink the boundary thickness. In second solution, it behaves in opposite approach. The force produced by the plate is not entirely moved to the liquid because of slip flow which allows an extra liquid to slip at the boundary. The micro rotation profile climbing with γ in both solutions as depicted in Figure 3(b). Alternatively, temperature distribution dwindles with growing γ for first solution and enhances for second solution as showed in Figure 3(c). Physically, because of slip parameter less amount of heat moved from the plate to the liquid and thus temperature distribution declines.

The velocity, micro rotation profiles and temperature distribution with micropolar parameter K are scrutinized in Figures 4(a)-(c) for water-based nanofluid. Figure 4(a) explains that the velocity boundary layer grows to be thicker and thicker because of growing values of K in both solutions. It is also clear that the velocity boundary layer is superior in case of non-Newtonian $(K \neq 0)$ compared to Newtonian fluid $(K = 0)$. Figure 4(b) indicates that the micro rotation profile shrinks with rising K in first and second solutions. Physically, because of increasing viscosity of microelements consequently constantly encourages slow down in the flow nearby the surface. Figure 4(c) illustrates that the temperature distribution enhances with higher values of K in both solutions.

Figures 5(a)-(c) are arranged to demonstrate the influence of modified Hartman number α on the velocity, micro rotation profiles and temperature distribution for water-based nanofluid. Figure 5(a) scrutinizes that the velocity rises because of growing values of α in first solution and declines in second solution. Physically, the values of α results in amplify external/internal forces as adhesive, electric forces, etc. In such forces, flow of momentum enhances and as a result velocity of fluid improves. Figure 5(b) reveals that the micro rotation confirms the decreasing behavior with growing values of α in both solutions. While Figure 5(c) explains that the temperature distribution diminish with larger values of α in first solution, reverse trend is captured in second solution. Physically, external/internal forces give an extra resistance to the motion of liquid particle. Consequently, extra heat is

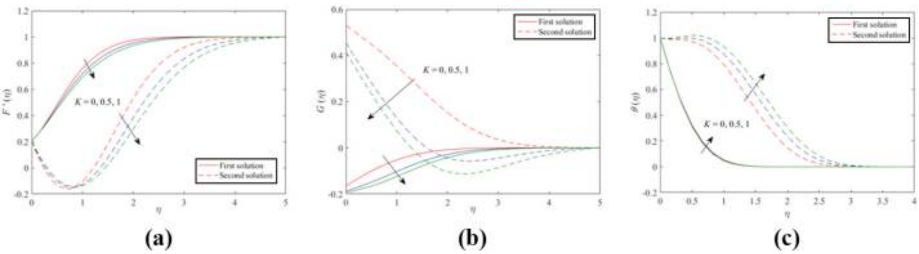

Figure 4.
Impact of K on (a) $F'(\eta)$ (b) $G(\eta)$ and (c) $\theta(\eta)$ when $\phi = 0.01$, $\gamma = 0.2$, $\lambda = -1.5$, $\alpha = 0.1$, $\Lambda = 1$

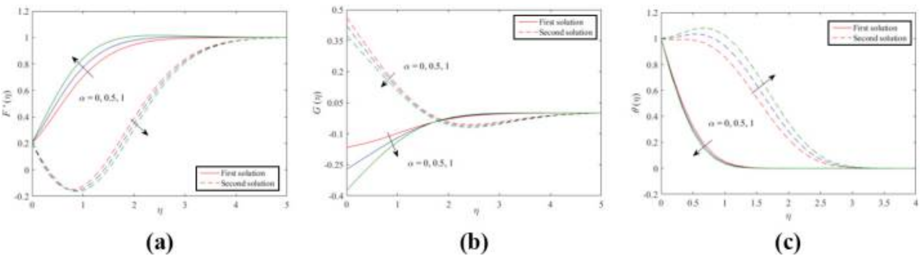

Figure 5.
Impact of α on (a) $F'(\eta)$ (b) $G(\eta)$ and (c) $\theta(\eta)$ when $\phi = 0.01$, $K = 0.5$, $\lambda = 0.2$, $\Lambda = 1$, $\lambda = -1.5$

created which in turns increases the temperature distribution in second solution. Figure 6(a) shows that the velocity shrinks with increasing dimensionless parameter Λ in first solution and boosts in second solution, whereas micro rotation shows an increasing pattern with growing Λ in first and second solutions. In contrast, temperature distribution enhances with growing Λ in first solution and diminishes in second solution as portrayed in Figure 6(c).

Figures 7(a) and (b) are placed to observe the performance of the skin friction and the Nusselt number vs. mixed convective parameter for preferred values of nanoparticle fraction for water and kerosene regular base fluids. Dual solutions are achieved for opposing flow, whereas the unique solution is found in assisting flow. The two different solutions were acquired by setting multiple guesses of η_∞, which generate two distinct profiles of velocity, micro rotation and temperature (Figures 2-6) where these satisfy the conditions (11) asymptotically and therefore might not be ignored. The multiple results exist up to some critical values of λ (say λ_c) and no solution exists for $\lambda > \lambda_c$. At $\lambda = \lambda_c$ the solution is unique, since branches of both solutions are connected. Based on computations, the values of λ_c are -3.2800 and -2.3295 for $\phi = 0.01$ and 0.02 in water-based fluid, whereas for kerosene-based fluid the values of λ_c are -1.7250 and -0.9770. Thus, the values of $|\lambda_c|$ decrease as nanoparticle fraction develop. Hence, the nanoparticle fraction accelerates the separation of boundary layer for water/kerosene-based fluids. Also, the critical values $|\lambda_c|$ of water-based fluid are larger compared to kerosene-based fluid, suggesting that the water-based fluid delays the boundary layer separation compared to kerosene-based fluid. Figures 7(a)-(b) indicate that the values of $C_{fx}\mathrm{Re}_x^{1/2}$ and $Nu_x\,\mathrm{Re}_x^{-1/2}$ enhances initially as ϕ growing and after $\lambda = 0$, it is starting to decrease in both solutions. Moreover, it is clear that all profiles interest at $\lambda = 0$ (buoyancy force absent). As Equations (8) and (10) are

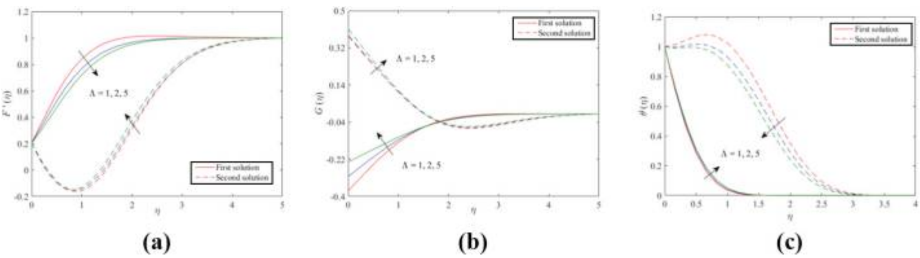

Figure 6. Impact of Λ on (a) $F'(\eta)$ (b) $G(\eta)$ and (c) $\theta(\eta)$ when $\phi = 0.01, K = 0.5, \lambda = 0.2, \alpha = 1, \lambda = -1.5$

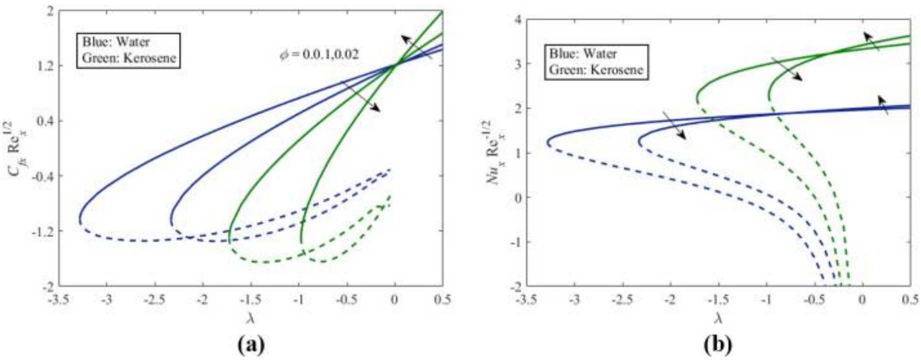

Figure 7. Impact of ϕ on (a) $C_{fx}\mathrm{Re}_x^{1/2}$ and (b) $Nu_x\mathrm{Re}_x^{-1/2}$ when $K = 0.5, \gamma = 0.2, \alpha = 0.1, \Lambda = 1$

decoupled, $\lambda = 0$. It is also explored from these figures that the values of $C_{fx}\,\mathrm{Re}_x^{1/2}$ and $Nu_x\,\mathrm{Re}_x^{-1/2}$ climb as mixed parameter enhances in case of assisting flow, whereas in opposing flow, the reverse trend is noticed. Physically, a favorable pressure gradient produces by assisting flow which improves the motion of fluid which consecutively enhances the rate of heat transfer and surface shear stress at the plate. In contrast, opposing flow guides an unfavorable pressure gradient which delays the flow and, thus, $C_{fx}\,\mathrm{Re}_x^{1/2}$ and $Nu_x\,\mathrm{Re}_x^{-1/2}$ decrease.

The influence of micropolar parameter on $C_{fx}\,\mathrm{Re}_x^{1/2}$ and $Nu_x\,\mathrm{Re}_x^{-1/2}$ versus λ is shown in Figures 8(a) and (b) for water and kerosene regular fluids. The values of $C_{fx}\,\mathrm{Re}_x^{1/2}$ raises with enhancing K in first solution and declines in second solution as depicted in Figure 8(a). Figure 8(b) shows that the values of $Nu_x\,\mathrm{Re}_x^{-1/2}$ decays initially and then after certain value of λ, it starting to increase as K progresses. Based on calculations, the values of λ_c are -3.0200 and -3.2800 for $K = 0$ and 0.5 in water-based fluid, whereas for kerosene-based fluid the values of λ_c are -1.5636 and -1.7250. Thus, the values of $|\lambda_c|$ increase as K expand for water/kerosene-based fluids. Hence, the micropolar parameter delays the separation of boundary layer for water/kerosene-based fluids. In contrast, the critical values $|\lambda_c|$ of kerosene-based fluid are smaller compared to water-based fluid, suggesting that micropolar parameter accelerates the separation of boundary layer for kerosene-based fluid. As expected, the Nusselt number is greater for kerosene-based fluid compared to water-based fluid because of higher thermal conductivity.

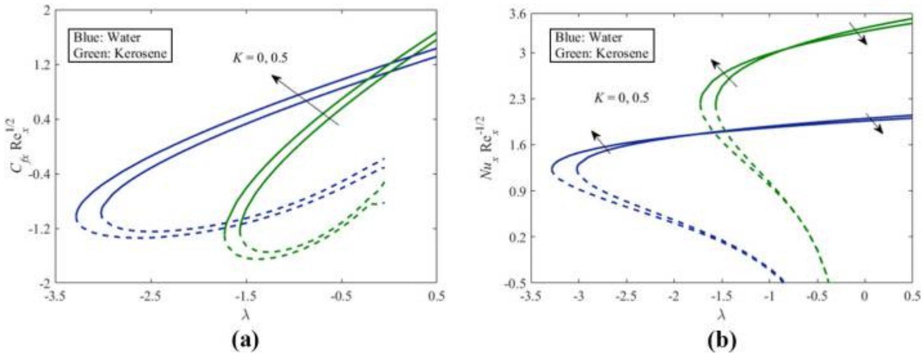

Figure 8.
Impact of K on (a) $C_{fx}\,\mathrm{Re}_x^{1/2}$ and (b) $Nu_x\mathrm{Re}_x^{-1/2}$ when $\phi = 0.01$, $\lambda = 0.2$, $\alpha = 0.1$, $\Lambda = -1$

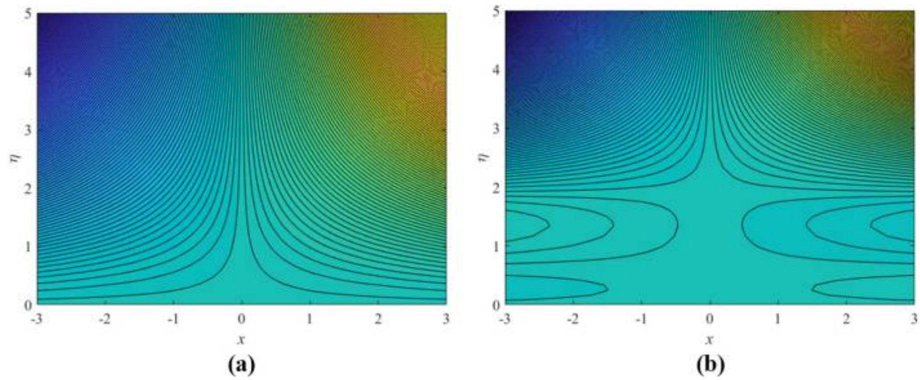

Figure 9.
Streamlines (a) First solution (b) Second solution when $K = 0.5$, $\phi = 0.01$, $\alpha = 0.1$, $\Lambda = 1$, $\lambda = -1.5$

The patterns of streamlines are presented in Figures 9(a) and (b) for first and second solutions. Figure 9(a) signifies that the streamlines are symmetric, simple and fuller towards an axis in first solution because of equal force of assisting and opposing flows. Alternatively, streamlines are slightly complicated in second solution and separated the flows in double region as shown in Figure 9(b).

Final remarks

In the present perusal, impact of partial slip on mixed convective micropolar fluid containing TiO_2-kerosene/water nanoparticles past a vertical Riga plate has been investigated. Similarity transformations have been applied to model the governing flow problem. The results of the governing flow problem are achieved through the Keller-box technique. The important outcomes for the current analysis are:

- Multiple solutions are obtained for opposing flow and certain value of mixed convection parameter, while the unique solution is obtained for assisting flow.
- The velocity profile declines with growing ϕ in first solution and advances in second solution, while conflicting performance is seen on temperature distribution. However, micro rotation profile rises in first and second solutions.
- Velocity and thermal boundary layers shrink because of slip parameter for first solution, while conflicting observation is perceived for second solution. Micro rotation profile describes the enhancing behavior in both solutions.
- Micropolar parameter decreases the fluid velocity and micro rotation profile in first and second solutions and leads to increase the temperature distribution in first and second solutions.
- Nanaoparticle volume fraction and micropolar parameter delay the boundary layer separation in water-based fluid and accelerate in kerosene-based fluid.
- Streamlines are fuller, symmetric and quite simple towards an axis in first solution and streamlines are slightly complicated and split the flow in two regions in second solution.

References

Abo-Eldahab, E.M. and El-Aziz, M.A. (2005), "Flow and heat transfer in a micropolar fluid past a stretching surface embedded in a non-Darcian porous medium with uniform free stream", *Applied Mathematics and Computation*, Vol. 162 No. 2, pp. 881-899.

Ahmad, A., Asghar, S. and Afzal, S. (2016), "Flow of nanofluid past a Riga plate", *Journal of Magnetism and Magnetic Materials*, Vol. 402, pp. 44-48.

Ahmed, S.E. and Rashad, A.M. (2016), "Natural convection of micropolar nanofluids in a rectangular enclosure saturated with anisotropic porous media", *Journal of Porous Media*, Vol. 19 No. 8, pp. 737-750.

Alsaedi, A., Awais, M. and Hayat, T. (2012), "Effects of heat generation/absorption on stagnation point flow of nanofluid over a surface with convective boundary conditions", *Communications in Nonlinear Science and Numerical Simulation*, Vol. 17 No. 11, pp. 4210-4223.

Aman, F. and Ishak, A. (2010), "Boundary layer flow and heat transfer over a permeable shrinking sheet with partial slip", *Journal of Applied Sciences Research*, Vol. 6 No. 8, pp. 111-115.

Aman, F., Ishak, A. and Pop, I. (2011), "Mixed convection boundary layer flow near stagnation-point on vertical surface with slip", *Applied Mathematics and Mechanics*, Vol. 32 No. 12, pp. 1599-1606.

Ashraf, M. and Bashir, S. (2012), "Numerical simulation of MHD stagnation point flow and heat transfer of a micropolar fluid towards a heated shrinking sheet", *International Journal for Numerical Methods in Fluids*, Vol. 69 No. 2, pp. 384-398.

Aziz, A., Khan, W.A. and Pop, I. (2012), "Free convection boundary layer flow past a horizontal flat plate embedded in porous medium filled by nanofluid containing gyrotactic microorganisms", *International Journal of Thermal Sciences*, Vol. 56, pp. 48-57.

Chamkha, A.J. and Rashad, A.M. (2014), "MHD forced convection flow of a nanofluid adjacent to a non-isothermal wedge", *Computational Thermal Sciences*, Vol. 6 No. 1, pp. 27-39.

Choi, S.U.S. (1995), "Enhancing thermal conductivity of fluids with nanoparticle", ASME Fluids Engineering Division, Vol. 231, pp. 99-106.

Das, K. (2012a), "Slip effects on heat and mass transfer in MHD micropolar fluid flow over an inclined plate with thermal radiation and chemical reaction", *International Journal for Numerical Methods in Fluids*, Vol. 70 No. 1, pp. 96-113.

Das, K. (2012b), "Slip effects on MHD mixed convection stagnation point flow of a micropolar fluid towards a shrinking vertical sheet", *Computers and Mathematics with Applications*, Vol. 63 No. 1, pp. 255-267.

Eastman, J.A., Cho, S.U.S., Li, S., Soyez, G., Thompson, L.J. and Dimelfi, R.J. (1999), "Novel thermal properties of nanostructured materials", *Journal of Metastable and Nanocrystalline Materials*, Vols 2/6, pp. 629-637.

El-Arabawy, H.A.M. (2003), "Effect of suction/injection on the flow of a micropolar fluid past a continuously moving plate in the presence of radiation", *International Journal of Heat and Mass Transfer*, Vol. 46 No. 8, pp. 1471-1477.

El-Kabeir, S.M.M., Chamkha, A.J. and Rashad, A.M. (2015), "Unsteady slip flow of a nanofluid due to a contracting cylinder with Newtonian heating", *Journal of Nanofluids*, Vol. 4 No. 3, pp. 394-401.

Ellahi, R. and Hameed, M. (2012), "Numerical analysis of steady non-Newtonian flows with heat transfer analysis, MHD and nonlinear slip effects", *International Journal of Numerical Methods for Heat and Fluid Flow*, Vol. 22 No. 1, pp. 24-38.

Eringen, A.C. (1966), "Theory of micropolar fluids", *Indiana University Mathematics Journal*, Vol. 16 No. 1, pp. 1-18.

Gailitis, A. and Lielausis, O. (1961), "On a possibility to reduce the hydrodynamic resistance of a plate in an electrolyte", *Applied Magnetohydrodynamics Reports on Physics Institute*, Vol. 12, pp. 143-146.

Ghalambaz, M., Nohgrehabadi, A. and Ghanbarzadeh, A. (2014), "Natural convection of nanofluids over a convectively heated vertical plate embedded in a porous medium", *Brazilian Journal of Chemical Engineering*, Vol. 31 No. 2, pp. 413-427.

Ghalambaz, M., Sabour, M. and Pop, I. (2016), "Free convection in a square cavity filled by a porous medium saturated by a nanofluid: Viscous dissipation and radiation effects", *Engineering Science and Technology, an International Journal*, Vol. 19 No. 3, pp. 1244-1253.

Gorla, R.S.R., El-Kabeir, S.M.M. and Rashad, A.M. (2011), "Boundary-layer heat transfer from a stretching circular cylinder in a naofluid", *Journal of Thermophysics and Heat Transfer*, Vol. 25 No. 1, pp. 183-186.

Hayat, T., Javed, T. and Abbas, Z. (2009), "MHD flow of a micropolar fluid near a stagnation-point towards a non-linear stretching surface", *Nonlinear Analysis: Real World Applications*, Vol. 10 No. 3, pp. 1514-1526.

Hussanan, A., Salleh, M.Z. and Khan, I. (2018), "Microstructure and inertial characteristics of a magnetite ferrofluid over a stretching/shrinking sheet using effective thermal conductivity model", *Journal of Molecular Liquids*, Vol. 255, pp. 64-75.

Iqbal, Z., Azhar, E., Mehmood, Z. and Maraj, E.N. (2017), "Melting heat transport of nanofluidic problem over a Riga plate with erratic thickness: use of keller box scheme", *Results in Physics*, Vol. 7, pp. 3648-3658.

Iqbal, Z., Azhar, E., Mehmood, Z. and Maraj, E.N. (2018), "Unique outcomes of internal heat generation and thermal deposition on viscous dissipative transport of viscoplastic fluid over a Riga-plate", *Communications in Theoretical Physics*, Vol. 69 No. 1, pp. 68-76.

Kelson, N.A. and Farrell, T.W. (2001), "Micropolar flow over a porous stretching sheet with strong suction or injection", *International Communications in Heat and Mass Transfer*, Vol. 28 No. 4, pp. 479-488.

Lok, Y.Y., Amin, N. and Pop, I. (2006), "Unsteady mixed convection flow of a micropolar fluid near the stagnation-point on a vertical surface", *International Journal of Thermal Sciences*, Vol. 45 No. 12, pp. 1149-1157.

Makinde, O.D. and Aziz, A. (2011), "Boundary layer flow of a nanofluid past a stretching sheet with a convective boundary condition", *International Journal of Thermal Sciences*, Vol. 53 No. 11, pp. 2477-2483.

Motsumi, T.G. and Makinde, O.D. (2012), "Effects of thermal radiation and viscous dissipation on boundary layer flow of nanofluids over a permeable moving flat plate", *Physica Scripta*, Vol. 86 No. 4, pp. 045003

Mustafa, M., Khan, J.A., Hayat, T. and Alsaedi, A. (2017), "Buoyancy effects on the MHD nanofluid flow past a vertical surface with chemical reaction and activation energy", *International Journal of Heat and Mass Transfer*, Vol. 108, pp. 1340-1346.

Nadeem, S., Haq, R.U. and Khan, Z.H. (2014), "Numerical study of MHD boundary layer flow of a Maxwell fluid past a stretching sheet in the presence of nanoparticles", *Journal of the Taiwan Institute of Chemical Engineers*, Vol. 45 No. 1, pp. 121-126.

Nohgrehabadi, A., Behseresht, A. and Ghalambaz, M. (2013a), "Natural-convection flow of nanofluid over vertical cone embedded in non-Darcy porous media", *Journal of Thermophysics and Heat Transfer*, Vol. 27 No. 2, pp. 334-341.

Nohgrehabadi, A., Ghalambaz, M. and Ghanbarzadeh, A. (2012b), "Heat transfer of magneto-hydrodynamic viscous nanofluids over an isothermal stretching sheet", *Journal of Thermophysics and Heat Transfer*, Vol. 26 No. 4, pp. 686-689.

Nohgrehabadi, A., Pourrajab, R. and Ghalambaz, M. (2012a), "Effect of partial slip boundary condition on the flow and heat transfer of nanofluids past stretching sheet prescribed constant wall temperature", *International Journal of Thermal Sciences*, Vol. 54, pp. 253-261.

Nohgrehabadi, A., Pourrajab, R. and Ghalambaz, M. (2013b), "Flow and heat transfer of nanofluids over stretching sheet taking into account partial slip and thermal convective boundary conditions", *Heat and Mass Transfer*, Vol. 49 No. 9, pp. 1357-1366.

Nohgrehabadi, A., Saffarian, M.R., Pourrajab, R. and Ghalambaz, M. (2013c), "Entropy analysis for nanofluid flow over a stretching sheet in the presence of heat generation/absorption and partial slip", *Journal of Mechanical Science and Technology*, Vol. 27 No. 3, pp. 927-937.

Pak, B.C. and Cho, Y.I. (1998), "Hydrodynamic and heat transfer study of dispersed fluids with submicron metallic oxide particles", *Experimental Heat Transfer*, Vol. 11 No. 2, pp. 151-170.

Pal, D., Mandal, G. and Vajravalu, K. (2016), "Soret and dufour effects on MHD convective–radiative heat and mass transfer of nanofluids over a vertical non-linear stretching/shrinking sheet", *Applied Mathematics and Computation*, Vol. 287-288, pp. 184-200.

Pantokratoras, A. (2011), "The blasius and sakiadis flows along a Riga-plate", *Progress in Computational Fluid Dynamics, An International Journal)*, Vol. 11 No. 5, pp. 329-333.

Pantokratoras, A. and Magyari, E. (2009), "EMHD free-convection boundary-layer flow from a Riga-plate", *Journal of Engineering Mathematics*, Vol. 64 No. 3, pp. 303-315.

Rashad, A.M. (2017a), "Impact of thermal radiation on MHD slip flow of a ferrofluid over a non-isothermal wedge", *Journal of Magnetism and Magnetic Materials*, Vol. 422, pp. 25-31.

Rashad, A.M. (2017b), "Unsteady nanofluid flow over an inclined stretching surface with convective boundary condition and anisotropic slip impact", *International Journal of Heat and Technology*, Vol. 35 No. 1, pp. 82-90.

Rashad, A.M., Chamkha, A.J. and Abdou, M.M.M. (2013), "Mixed convection flow of non-Newtonian fluid from vertical surface saturated in a porous medium filled with a nanofluid", *Journal of Applied Fluid Mechanics*, Vol. 6 No. 2, pp. 301-309.

Rashid, I., Haq, R.U., Khan, Z.H. and Al-Mdallal, Q.M. (2017), "Flow of water based alumina and copper nanoparticles along a moving surface with variable temperature", *Journal of Molecular Liquids*, Vol. 246, pp. 354-362.

Shah, R.A., Abbas, T., Idrees, M. and Ullah, M. (2017), "MHD Carreau fluid slip flow over a porous stretching sheet with viscous dissipation and variable thermal conductivity", *Boundary Value Problem*, Vol. 2017, p. 94

Sivasankaran, S., Mansour, M.A., Rashad, A.M. and Bhuvaneswari, M. (2016), "MHD mixed convection of Cu–water nanofluid in a two-sided lid-driven porous cavity with a partial slip", *Numerical Heat Transfer, Part A: Applications*, Vol. 70 No. 12, pp. 1356-1370.

Tahmasebi, A., Mahdavi, M. and Ghalambaz, M. (2018), "Local thermal nonequilibrium conjugate natural convection heat transfer of nanofluids in a cavity partially filled with porous media using buongiorno's model", *Numerical Heat Transfer, Part A: Applications*, Vol. 73 No. 4, pp. 254-276.

Wang, C.Y. (2009), "Analysis of viscous flow due to a stretching sheet with surface slip and suction", *Nonlinear Analysis: Real World Applications*, Vol. 10 No. 1, pp. 375-380.

Waqas, M., Farooq, M., Khan, M.I., Alsaedi, A., Hayat, T. and Yasmeen, T. (2016), "Magnetohydrodynamic (MHD) mixed convection flow of micropolar liquid due to nonlinear stretched sheet with convective condition", *International Journal of Heat and Mass Transfer*, Vol. 102, pp. 766-772.

Zaib, A. and Shafie, S. (2015), "Slip effect on an unsteady MHD stagnation-point flow of a micropolar fluid towards a shrinking sheet with thermophoresis effect", *International Journal for Computational Methods in Engineering Science and Mechanics*, Vol. 16 No. 5, pp. 285-291.

Zaib, A., Bhattacharyya, K. and Shafie, S. (2016), "Effect of partial slip on an unsteady MHD mixed convection stagnation-point flow of a micropolar fluid towards a permeable shrinking sheet", *Alexandria Engineering Journal*, Vol. 55, pp. 1285-1293.

Zargartalebi, H., Ghalambaz, M., Khanafer, K. and Pop, I. (2017), "Unsteady conjugate natural convection in a porous cavity boarded by two vertical finite thickness walls", *International Communications in Heat and Mass Transfer*, Vol. 81, pp. 218-228.

Corresponding author
Aurang Zaib can be contacted at: zaib20042002@yahoo.com